Toxicology and Applied Pharmacology 286 (2015) 178–187

Contents lists available at ScienceDirect

Toxicology and Applied Pharmacology

journal homepage: www.elsevier.com/locate/ytaap

Enhancement of endocannabinoid signaling protects against cocaine-induced neurotoxicity

Luciano R. Vilela [a], Pedro H. Gobira [b], Thercia G. Viana [b], Daniel C. Medeiros [c], Talita H. Ferreira-Vieira [c], Juliana G. Doria [a], Flávia Rodrigues [d], Daniele C. Aguiar [b], Grace S. Pereira [c], André R. Massessini [c], Fabíola M. Ribeiro [d], Antonio Carlos P. de Oliveira [b], Marcio F.D. Moraes [c,*,1], Fabricio A. Moreira [b,*,1]

[a] Graduate Program in Neuroscience, Institute of Biological Sciences, Universidade Federal de Minas Gerais, Belo Horizonte, MG, Brazil
[b] Department of Pharmacology, Institute of Biological Sciences, Universidade Federal de Minas Gerais, Belo Horizonte, MG, Brazil
[c] Department of Physiology, Institute of Biological Sciences, Universidade Federal de Minas Gerais, Belo Horizonte, MG, Brazil
[d] Department of Biochemistry and Immunology, Institute of Biological Sciences, Universidade Federal de Minas Gerais, Belo Horizonte, MG, Brazil

ARTICLE INFO

Article history:
Received 9 February 2015
Revised 15 April 2015
Accepted 21 April 2015
Available online 29 April 2015

Keywords:
Endocannabinoid
Anandamide
FAAH
Cocaine
Seizures
PI3K

ABSTRACT

Cocaine is an addictive substance with a potential to cause deleterious effects in the brain. The strategies for treating its neurotoxicity, however, are limited. Evidence suggests that the endocannabinoid system exerts neuroprotective functions against various stimuli. Thus, we hypothesized that inhibition of fatty acid amide hydrolase (FAAH), the main enzyme responsible for terminating the actions of the endocannabinoid anandamide, reduces seizures and cell death in the hippocampus in a model of cocaine intoxication. Male Swiss mice received injections of endocannabinoid-related compounds followed by the lowest dose of cocaine that induces seizures, electroencephalographic activity and cell death in the hippocampus. The molecular mechanisms were studied in primary cell culture of this structure. The FAAH inhibitor, URB597, reduced cocaine-induced seizures and epileptiform electroencephalographic activity. The cannabinoid CB_1 receptor selective agonist, ACEA, mimicked these effects, whereas the antagonist, AM251, prevented them. URB597 also inhibited cocaine-induced activation and death of hippocampal neurons, both in animals and in primary cell culture. Finally, we investigated if the PI3K/Akt/ERK intracellular pathway, a cell surviving mechanism coupled to CB_1 receptor, mediated these neuroprotective effects. Accordingly, URB597 injection increased ERK and Akt phosphorylation in the hippocampus. Moreover, the neuroprotective effect of this compound was reversed by the PI3K inhibitor, LY294002. In conclusion, the pharmacological facilitation of the anandamide/CB1/PI3K signaling protects the brain against cocaine intoxication in experimental models. This strategy may be further explored in the development of treatments for drug-induced neurotoxicity.

Introduction

Addiction is a major public health problem with a high prevalence worldwide. Among the most commonly addictive drugs is cocaine, a psychostimulant and psychotomimetic compound (Degenhardt and Hall, 2012), which may induce acute and chronic psychiatric and neurological effects, including psychosis, agitation and seizures (Cadet et al., 2014). The molecular targets underlying cocaine-induced psychosis and behavioral stimulation include inhibition of neuronal monoamine uptake, particularly dopamine (Wise, 1984; Koob and Nestler, 1997). Accordingly, these effects are reversed by antipsychotic drugs, mainly through antagonism at dopamine D_2 receptor (Kishi et al., 2013). The mechanisms underlying the neurotoxic effects of this drug are less understood, since several intracellular biochemical processes seem to be involved (Cunha-Oliveira et al., 2008; Planeta et al., 2013). Thus, experimental models of cocaine intoxication are relevant for studying its biological mechanisms as well as new treatment approaches (Connors and Hoffman, 2013; Heard et al., 2011).

One possible strategy to reduce cocaine-induced neural damage would be facilitating protective mechanisms already at play in the brain. In this context, the endocannabinoid system has been proposed as an on-demand defense mechanism against neural hyper-excitability (Lutz, 2004; van der Stelt and Di Marzo, 2005; Fowler et al., 2010). This

Abbreviations: Akt, protein kinase B; CB_1, cannabinoid type-1 receptor; CB_2, cannabinoid type-2 receptor; D2, dopamine type-2 receptor; Δ^9-THC, Δ^9-tetrahydrocannabinol; EEG, electroencephalography; ERK, extracellular signal-regulated kinase; FAAH, fatty acid amide hydrolase; PI3K, phosphoinositide 3-kinase; TRPV1, transient receptor potential type-1 channel.

* Corresponding authors at: Institute of Biological Sciences, Universidade Federal de Minas Gerais, Av. Antônio Carlos 6627, 31270-901, Belo Horizonte, MG, Brazil. Fax: +55 31 3409 2924.
E-mail addresses: mfdm@icb.ufmg.br (M.F.D. Moraes), fabriciomoreira@icb.ufmg.br (F.A. Moreira).

[1] These authors share senior authorship.

http://dx.doi.org/10.1016/j.taap.2015.04.013
0041-008X/

system is named after the *Cannabis sativa*, a plant whose main active constituent is Δ^9-tetrahydrocannabinol (Δ^9-THC). The typical components of the endocannabinoid system are the cannabinoid CB_1 and CB_2 receptors, their endogenous agonists (endocannabinoids), among which are arachidonoyl ethanolamide (anandamide) and 2-arachidonoyl glycerol; and the mechanisms mediating their synthesis and hydrolysis (Piomelli, 2003). The primary enzyme responsible for terminating anandamide actions is fatty acid amide hydrolase (FAAH) (Cravatt et al., 1996). Specific compounds have been developed to inhibit this enzyme and facilitate endocannabinoid signaling (Kathuria et al., 2003).

Cannabinoids and the endocannabinoid system have been investigated mainly in relation to their effects upon cocaine self-administration and psychomotor stimulation (Panlilio et al., 2010; Xi and Gardner, 2008; Moreira et al., 2015). Anandamide, however, is synthesized and release particularly in response to excessive neural activity, providing on-demand protection though CB_1 receptor signaling in the hippocampus (Marsicano et al., 2003; Monory et al., 2006). Moreover, compounds that inhibit anandamide hydrolysis induce neuroprotective effects (Karanian et al., 2007; Slusar et al., 2013) and attenuate seizures and electroencephalographic (EEG) activity induced by experimental convulsant substances (Karanian et al., 2007; Vilela et al., 2013, 2014). Thus, it is reasonable to suppose that CB_1 receptor activation also protects against cocaine toxicity. Indeed, one study observed that cannabinoids reduce seizures induced by various substances, including cocaine (Hayase et al., 2001). In spite of this evidence, the effects of anandamide hydrolysis inhibition upon cocaine neurotoxicity have not been investigated. Importantly, compounds acting through this mechanism facilitate the on-demand actions of anandamide and therefore have low propensity to induce motor impairment and other deleterious outcomes. This is in contrast to Δ^9-THC and other cannabinoids, which directly activate the CB_1 receptor and lack spatial and temporal resolution in their actions (Moreira and Wotjak, 2010).

The CB_1 receptor is coupled to diverse intracellular signaling pathways, including the phosphoinositide 3-kinase/protein kinase B/extracellular signal-regulated kinase (PI3K/Akt/ERK) pathway, which is known to exert neuroprotective functions (Galve-Roperh et al., 2002; Ozaita et al., 2007). Considering these pieces of evidence, we hypothesized that facilitating anandamide actions confers protection against cocaine excitotoxic through recruitment of the intracellular PI3K/Akt/ERK pathway in the hippocampus. Thus, we tested the effects of FAAH inhibition against seizures, EEG activity and hippocampal cell death in an experimental model of acute cocaine intoxication. To investigate the role of the CB_1 receptor/PI3K/Akt/ERk pathway, we performed experiments with selective compounds both in animals and in hippocampal cell culture.

Methods

Animals. Male Swiss mice (20–30 g) from the animal facility of the Federal University of Minas Gerais were kept on a 12 h:12 h dark/light cycle at 22 ± 1 °C with free access to food and water. All efforts were made to minimize animal suffering and to employ the least number of animals in each experiment. The protocols are in accordance with the Ethical Committee for Animal Experimentation (CETEA) of this University (Protocol 242/2013), which follows the Brazilian law no. 11.794/2008 and are in accordance with the international statement on the requirement for research involving animals (The Basel Declaration) and the Concordat on Openness on Animal Research.

Chemicals and injection protocols. The following compounds were used: The selective FAAH-inhibitor, [3-(3-carbamoylphenyl)phenyl]N-cyclohexylcarbamate (URB597); the CB_1 receptor selective agonist arachidonoyl chloroethylamide (ACEA); the CB_1 receptor antagonist/inverse agonist, 1-(2,4-dichlorophenyl)-5-(4-iodophenyl)-4-methyl-N-1-piperidinyl-1H-pyrazole-3 carboxamide (AM251). They were purchased from Cayman Chemical Company (1180 East Ellsworth Road, Ann Arbor, Michigan 48108, USA) and suspended in ethanol/cremophor (Sigma)/0.9% saline (1:1:18). Cocaine hydrochloride (Merck, Whitehouse Station, New Jersey, USA) was dissolved in saline; and the PI3K inhibitor 2-morpholin-4-yl-8-phenylchromen-4-one (LY294002; Tocris, Tocris House, IO Centre, Moorend Farm Ave, Bristol, Avon BS11 0QL, UK), was dissolved in DMSO 1% with a final concentration of 0.1%. All compounds have purity higher than 98%, as informed by each supplier. Rabbit anti-phospho Akt, anti-phospho ERK1/2, anti-Akt and anti-ERK1/2 monospecific clonal antibodies were from DB Biotech (Kosice, Slovakia). All injections were performed intraperitoneally (i.p.) in a volume of 1 ml kg^{-1}.

Surgery. The animals were anesthetized with ketamine (60 mg kg^{-1}) and xylazine (8 mg kg^{-1}) and positioned in a stereotaxic frame (David Kopf model 960). Stainless steel bone-screw electrodes (Fine Sciences Tools, mod. 19010-00) were placed over parietal cortices and fixed to the skull with zinc cement and soldered to pin bars. Coordinates (AP = 2.0 mm, ML = ± 2.0 mm referenced from the bregma suture) were derived from a stereotaxic atlas for mice (Paxinos and Watson, 1997). A reference electrode was inserted into the nasal bone. The animals received prophylactic intramuscular injections of polyantibiotic (0.27 g kg^{-1}; benzylpenicillin, streptomycin and dihydrostreptomycin Pentabiotico®, Fort Dodge, Brazil) and the nonsteroidal anti-inflammatory drug flunixinmeglumine (0.025 g kg^{-1}; Banamine®, Schering Plough, Brazil). They were allowed to recover for 4–5 days before the experiments.

Cocaine-induced seizures. For quantification of seizures, the animals received cocaine injections and were immediately placed in individual chambers for 10 min in an isolated room. The lowest seizure-inducing dose of cocaine was selected based on a dose–response curve. Seizure was defined as the occurrence of tail clonus with myoclonic jerks and wild jumping or convulsions with loss of righting reflex (Gasior et al., 1999; Vilela et al., 2013). An experimenter, unaware of the treatments, quantified the latency and duration of seizures. Vehicle or URB597 were administered 30 min before cocaine. The CB_1 receptor antagonist AM251 was administered 10 min before URB597.

Electroencephalografic recording and analysis. Video-EEG recordings were performed starting 1 min before cocaine administration until 30 s after the seizures onset. The EEG signal was amplified (5000×), filtered (1 Hz high pass and 500 Hz low pass) and digitized using an A/D converter set at a sampling rate of 1 kHz (Aisha4 Kananda® Ltda, Belo Horizonte, MG, Brazil); the data were stored in a personal computer. The records were analyzed off-line according to the latency to the onset and the duration of the epileptiform discharge (Vilela et al., 2013).

Fos immunohistochemistry. Two hours after cocaine administration, animals were anesthetized with an overdose of urethane and perfused transcardially with saline (200 nl) followed by 4% paraformaldehyde (PFA 4%) in 0.1 M phosphate buffer (150 ml, pH 7.4). Brains were removed and post fixed over 2 h in PFA 4% and stored for 36 h in 30% sucrose for cryoprotection. Coronal sections (40 μm) were obtained in a cryostat in triplicate for imunohystochemistry, as previously described (Beijamini and Guimarães, 2006). Briefly, tissue sections were washed with phosphate buffer in saline (PBS) and incubated overnight at room temperature with rabbit IgG in PBS (1:1000). The sections were washed in PBS and incubated with a biotinilated anti-rabbit IgG (1:1000). Fos immunoreactivity was revealed by the addition of the chromogen diaminobenzidin (DAB, from Sigma) and visualized as a brown precipitate inside the neuronal nuclei.

Cell death in the hippocampal tissue from cocaine-treated animals. The animals were killed by cervical displacement 24 h after cocaine injections. Their brains were rapidly (<1 min) removed and submerged in cold (2–3 °C) ACSF (artificial cerebrospinal fluid) solution: (in mM)

125 NaCl, 2.5 KCl, 2 $CaCl_2$, 1 $MgCl_2$, 25 $NaHCO_3$, 1.25 NaH_2PO_4, 25 glucose bubbled with 95% O2, 5% CO2, PH 7.4. In addition, the brain was placed in inside the vibratome (Vibratome, Series 1000, Technical Products International) and was cut in transverse slices (400 μm) containing the hippocampal formation (Leite et al., 2012). For the analysis of cell viability, the slices were incubated with 6 mM ethidium homodimer (live/dead assay, Molecular Probes, Inc.) for 30 min, then washed for 15 min in 2 ml of 95% O_2/5% CO_2 ACSF at room temperature. After, the slices were fixed in paraformaldehyde 4% for 15 min, washed for 5 min in PBS and again washed in ACSF. During the staining procedure the slices were protected from light. Dead cells were indicated by the red fluorescence of ethidium homodimer. Images were acquired using a fluorescence microscope Axio Imager.M2 - Zeiss system using 10× objective. Fluorescence images showing specific red-fluorescent nucleic acid staining of dead cells were collected. We used the Carl Zeiss Axiovision 4.8 software to acquire and create images reconstructions. To improve images for quantitative analysis, they were processed using the median filter. In the current approach, we define nucleus as connected pixels that were above a threshold. This threshold was calculated using the image histogram, and the pixels below the threshold were set to 0. Slices containing CA1 and DG region of the hippocampus were selected and analyzed using the Image J software to calculate the percentage of threshold area in the image which, indirectly, reflects the number of dead cells.

Immunoblotting for Akt and ERK1/2. To investigate drug effects upon Akt and ERK1/2 phosphorylation, the hippocampi were dissected and lysed in Triton buffer (1% Triton X-100, 0.15 M NaCl, 0.05 M Tris–HCl, pH 7.2) containing protease inhibitors (1.0 mM AEBSF and 10.0 μg/ml of both leupeptin and aprotinin). An amount of 100.0 μg of total cellular protein for each sample was subjected to SDS-PAGE, followed by electroblotting onto nitrocellulose membranes. Membranes were blocked with 5% BSA in wash buffer (150.0 mM NaCl, 10.0 mM Tris–HCl, pH 7.0 and 0.05% Tween 20) for 1 h and then incubated with either rabbit anti-phosphoAkt (S473) or anti-phospho ERK1/2 (Thr202/Thr204) (1:1000) antibodies in wash buffer containing 3% BSA for 2 h at room temperature. Membranes were rinsed three times with wash buffer and then incubated with secondary HRP-conjugated goat anti-rabbit IgG diluted 1:5000 in wash buffer containing 3% skim milk for 1 h. Later, they were incubated with ECL Western blotting detection reagents. Antibodies were then stripped and membranes were incubated with either anti-Akt or anti-ERK1/2 (1:1000) for 2 h and probed with secondary antibody to determine total Akt and ERK1/2 expression. Nonsaturated, immunoreactive Akt and ERK1/2 bands were quantified by scanning densitometry. Immuno-band intensity was calculated using ImageJ TM software. The number of pixels of Akt phospho-bands and ERK1/2 phospho-bands were divided by the number of pixels of total Akt and ERK1/2, respectively, to normalize the levels of phosphorylated kinases to total kinase expression (Doria et al., 2013; Ribeiro et al., 2010). The treatment groups were compared to the basal levels (vehicle groups) of phosphorylation, which is presented as 100% values.

Cell death in primary culture of the hippocampus. Neuronal cultures were prepared from the hippocampus region of C57 mouse embryo brains at the embryonary day 19. The purity of the cell culture was determined by NeuN staining, which was expressed in 95% of the cell as being classified as neurons (Doria et al., 2013). After dissection, the tissue was submitted to trypsin digestion followed by cell dissociation using a fire-polished Pasteur pipette. Cells were plated on poly-L-ornithine-coated dishes in neurobasal medium supplemented with N2 and B27 supplements, 2.0 mM GlutaMAX, 50.0 mg/ml penicillin and 50.0 mg/ml streptomycin. Cells were incubated at 37 °C and 5% CO_2 in a humidified incubator and cultured for 10–12 days *in vitro* with medium replenishment every 4 days.

For the cell death assay, the plates were incubated for 20 h with either vehicle or cocaine (from a 25 μM to 1000 μM) combined with URB597, AM251 and LY294002. Cell death was determined by a live/dead viability assay, as described previously (Ribeiro et al., 2010). Briefly, neurons were stained with 2.0 mM calceinacetoxymethyl ester (AM) and 2.0 mM ethidium homodimer-1 for 15 min and the fractions of live (calcein AM positive) and dead (ethidium homodimer-1 positive) cells were determined. The cells were visualized by fluorescence microscopy EVOS® FLOID® Cell Imaging Station (Life Technologies, Carlsbad, CA, USA) and scored by a blinded observer. A minimum of 300 cells were analyzed per well in triplicate using ImageJ software. Dead cells were expressed as a percentage of the total number of cells (Doria et al., 2013).

Data analysis. The dependent variables were subjected to one- or two-way ANOVA, as appropriate, followed by Newman–Keuls post hoc test. Data are presented as mean ± SEM. The significance level was considered at $p < 0.05$. The statistical software used was the GraphPad Prism 5.0 Version for Windows (San Diego, CA, USA).

Results

URB597, an anandamide hydrolysis inhibitor, reduces cocaine-induced seizures in mice

The first experiment consisted of a dose–response curve for selecting the lowest dose of cocaine able to induce seizures in mice. Administration of cocaine at doses of 75 and 100 mg kg^{-1} induced seizures, as revealed by their latency ($F_{3,20} = 81.99$, $p < 0.0001$; Fig. 1A) and duration ($F_{3,24} = 14.81$, $p < 0.0001$; Fig. 1B). Next, we investigated whether URB597 (0.3, 1.0 and 3.0 mg kg^{-1}) could reduce cocaine-induced seizures. This substance was effective, at the dose of 1.0 mg kg^{-1}, in both increasing seizure latency ($F_{3,28} = 5.779$, $p = 0.003$; Fig. 1C) and reducing seizure duration ($F_{3,28} = 3.853$, $p = 0.02$; Fig. 1D). This effect was confirmed in an independent experiment by treating animals with the CB1 receptor selective agonist, ACEA (1, 2 and 4 mg kg^{-1}), which increased seizure latency at the intermediate dose ($F_{3,27} = 3.761$, $p = 0.02$; Fig. 1E), although the effects upon seizure duration did not reach significance ($F_{3,27} = 1.245$, ns; Fig. 1F).

The protective effects of URB597 against cocaine-induced seizures and electroencephalografic activity are mediated by the CB_1 receptor

We tested the hypothesis that the effects of URB597 would be prevented by a CB_1 receptor antagonist. As in the previous experiment, URB597 inhibited the effects of cocaine, increasing seizure latency and decreasing duration. AM251, at the dose of 1.0 mg kg^{-1} reversed the anticonvulsant effect of URB597 for both latency ($F_{3,27} = 8.325$, $p = 0.001$; Fig. 2A) and duration ($F_{3,27} = 3.359$, $p = 0.04$; Fig. 2B) of seizures. These behavioral results were paralleled by the effects of these drugs upon EEG recordings. AM251 reversed the effects of URB597 upon cocaine-induced EEG activity latency ($F_{3,20} = 8.538$,$p = 0.002$; Fig. 2C) and duration ($F_{3,21} = 5.718$, $p = 0.01$; Fig. 2D). This dose of AM251 was ineffective by itself (data not shown). Representative recordings of EEG activity after each treatment are presented in Fig. 3.

URB597 inhibits cocaine-induced c-Fos protein expression the hippocampus

We hypothesized that the CA1 region and dentate gyrus of the hippocampus are related to cocaine-induced seizures, considering the role of these regions in elaborating ictal activity. Indeed, immunostaining with c-Fos antibody indicated a significant increase in the number of Fos-positive cells in the CA1 region of hippocampus in cocaine-treated animals, which was abolished by URB597. There was no overall effect of URB597 ($F_{1,15} = 0.923$, ns); a significant cocaine effect ($F_{1,15} = 9.101$, $p = 0.0087$) and a interaction between factor ($F_{1,15} = 7.802$;

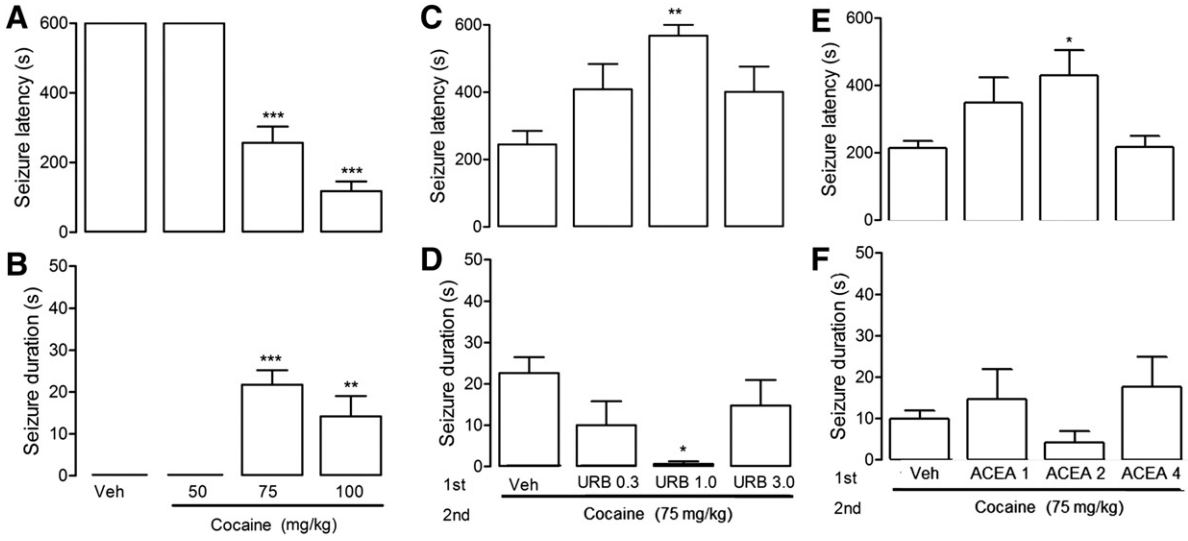

Fig. 1. Effects of cocaine and pre-treatments with URB597 and ACEA on seizures in mice. (A, B) Cocaine induced seizure as quantified by their latency and duration in comparison to vehicle-treated animals. (C, D) The anandamide hydrolysis inhibitor, URB597, inhibited cocaine-induced seizures. (E, F) The CB_1 receptor selective agonist, ACEA, also attenuated cocaine-induced seizures. $^{*}p < 0.05$, $^{**}p < 0.01$ and $^{***}p < 0.001$ compared to the respective vehicle (Veh) groups; one-way ANOVA followed by Newman–Keuls test. Data are expressed as mean ± SEM (n = 6–9, n = 8–11 and n = 7–8 per group).

$p = 0.0136$). Post-hoc analysis indicated that cocaine increased c-Fos expression and URB597 selective prevented this effect (Fig. 4A). No alteration, however, was found in the dentate gyrus. There was no effect of URB597 treatment ($F_{1,15} = 0.5116$, ns) or cocaine ($F_{1,15} = 0.1161$, ns) and no interaction between factors ($F_{1,15} = 0.4645$, ns), as shown in Fig. 4B. Altogether, these results suggest that reductions in cocaine-induced neuronal activation in CA1 region of hippocampus may contribute for the anticonvulsant effect of URB597. Representative photomicrographies of Fos- positive cells can be seen in Fig. 4C–F.

URB597 inhibits cocaine-induced cell death in the hippocampus

In the next set of experiments, we sought to determine whether a pre-treatment with URB597 would also protect against cell death in

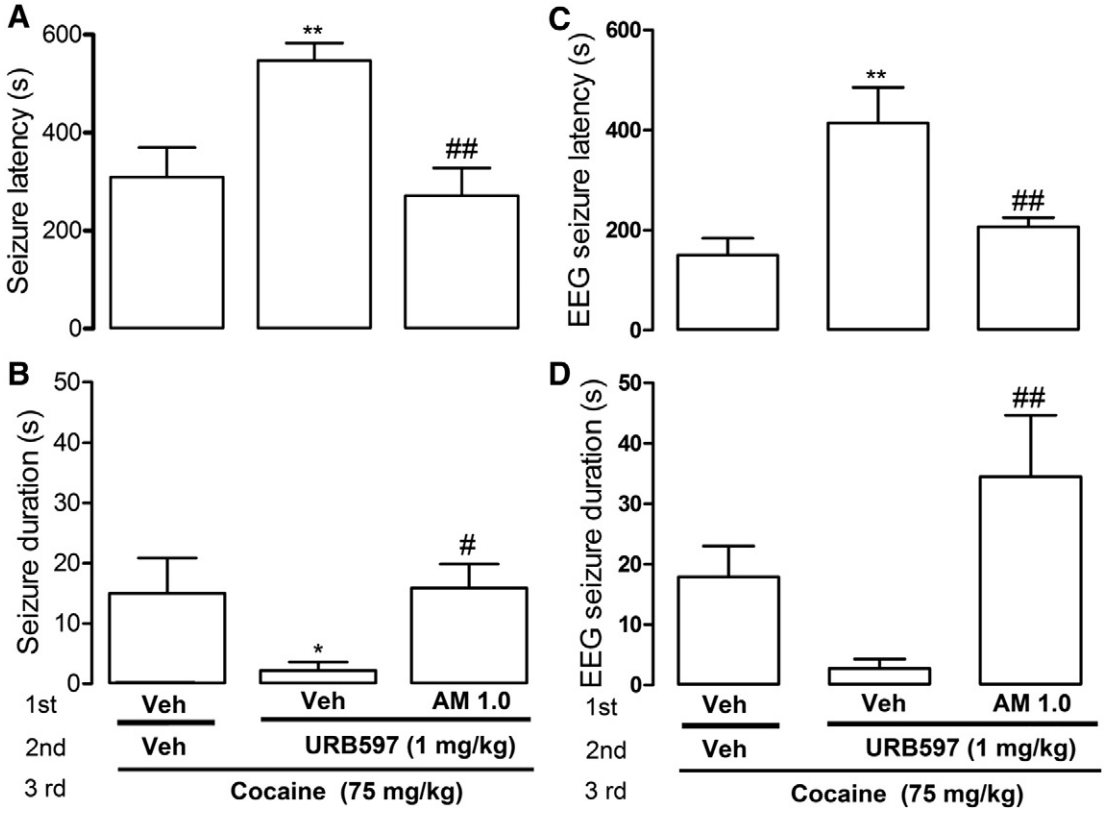

Fig. 2. Role of CB_1 receptor in the protective effects of URB597 against cocaine-induced seizures and EEG activity in mice. (A, B) Pre-treatment with the CB_1 receptor antagonist, AM251, reversed the protective effects of URB597 on cocaine-induced seizures. (C, D) These effects were paralleled by effects on EEG-activity. $^{*}p < 0.05$ and $^{**}p < 0.01$ compared to vehicle + vehicle (Veh) group; $^{\#}p < 0.05$ and $^{\#\#}p < 0.01$ compared to Veh + URB597 group; one-way ANOVA followed by Newman–Keuls test. Data are expressed as mean ± SEM (n = 10 mice/group).

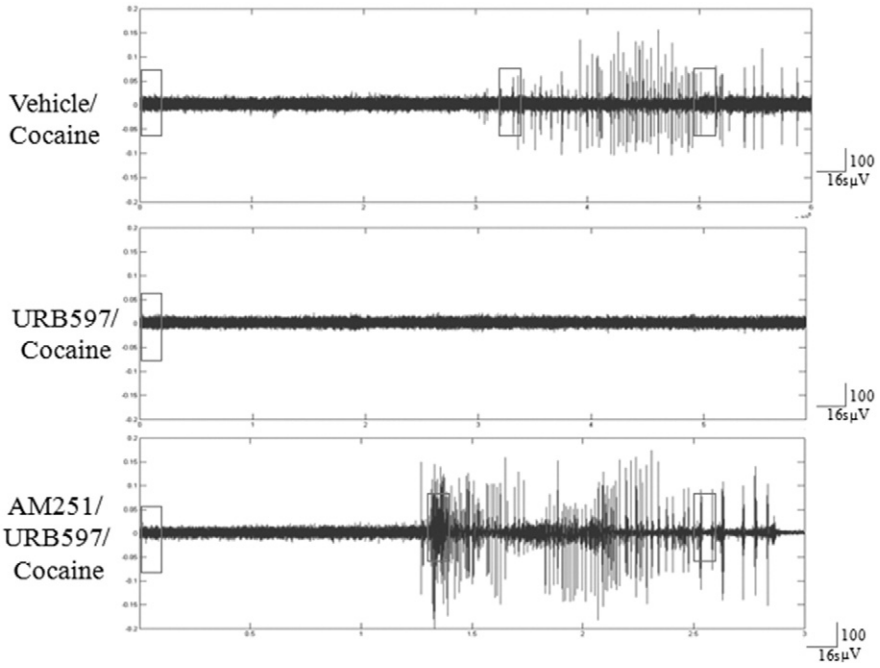

Fig. 3. Representative EEG recordings for AM251 (1 mg/kg), URB597 (1 mg/kg) and cocaine (75 mg/kg) treated mice. Vertical bars show the beginning of recording and the beginning and end of seizures activity.

the hippocampus of cocaine-treated animals. There was an increase of cell death in CA1 region and dentate gyrus of hippocampus defined by higher fluorescence of these areas. URB597 significantly attenuated overall hippocampal cell death in CA1 region. There was no effect of URB597 factor ($F_{1.18} = 0.3645$, ns); as expected, there was an overall effect of cocaine in increasing cell death ($F_{1.18} = 11.13$; 0.0037); and there was an interaction between factors ($F_{1.18} = 3.608$; 0.0474), with post-hoc analysis showing that URB597 prevented cocaine-induced cell death (Fig. 5A). A similar profile has been observed in the dentate gyrus. There was no overall effect of URB597 ($F_{1.18} = 2.922$, ns), there was a cocaine effect ($F_{1.18} = 5.972$, $p = 0.0291$) and an interaction between factors ($F_{1.18} = 8.065$, $p = 0.0109$), again with post-hoc analysis indicating that URB597 also protected against cell death in this part of the hippocampus (Fig. 5B). Representative images of ethidum bromide staining for each group are depicted in Fig. 5C–J.

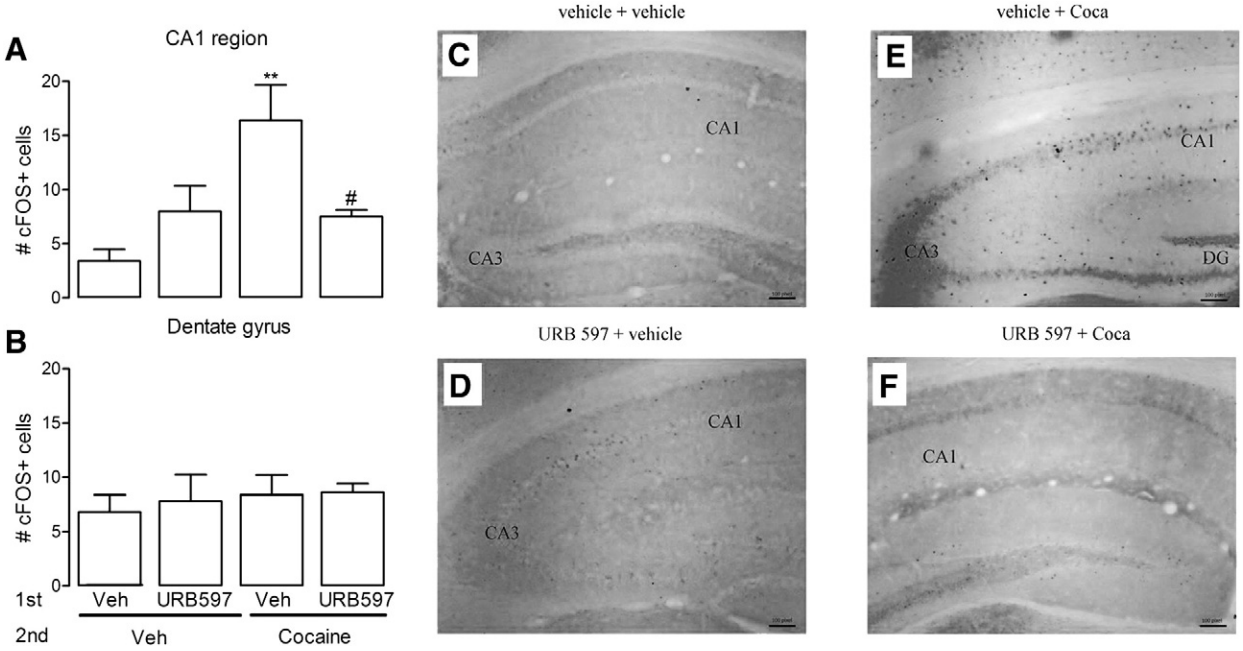

Fig. 4. Effects of the anandamide hydrolysis inhibitor, URB597 (1 mg kg^{-1}), on cocaine (75 mg kg^{-1})-induced cFos expression in the CA1 and dentate gyrus regions of the mouse hippocampus 2 h after the convulsive seizures. (A) URB597 reduced cocaine-induced cFos expression in the CA1. (B) No change was observed in the dentate gyrus. (C–F) Representative photomicrographies of cFos-positive cells in the hippocampus (coronal sections, 40 μm) for each experimental group. Bar size: 100 μm. Magnification = 20×. $^{**}p < 0.01$ compared to vehicle-vehicle (Veh) group; $^{\#\#}p < 0.01$ compared to Veh + cocaine group; one-way ANOVA followed by Newman–Keuls test. Data are expressed as mean ± SEM (n = 4–5 mice/group).

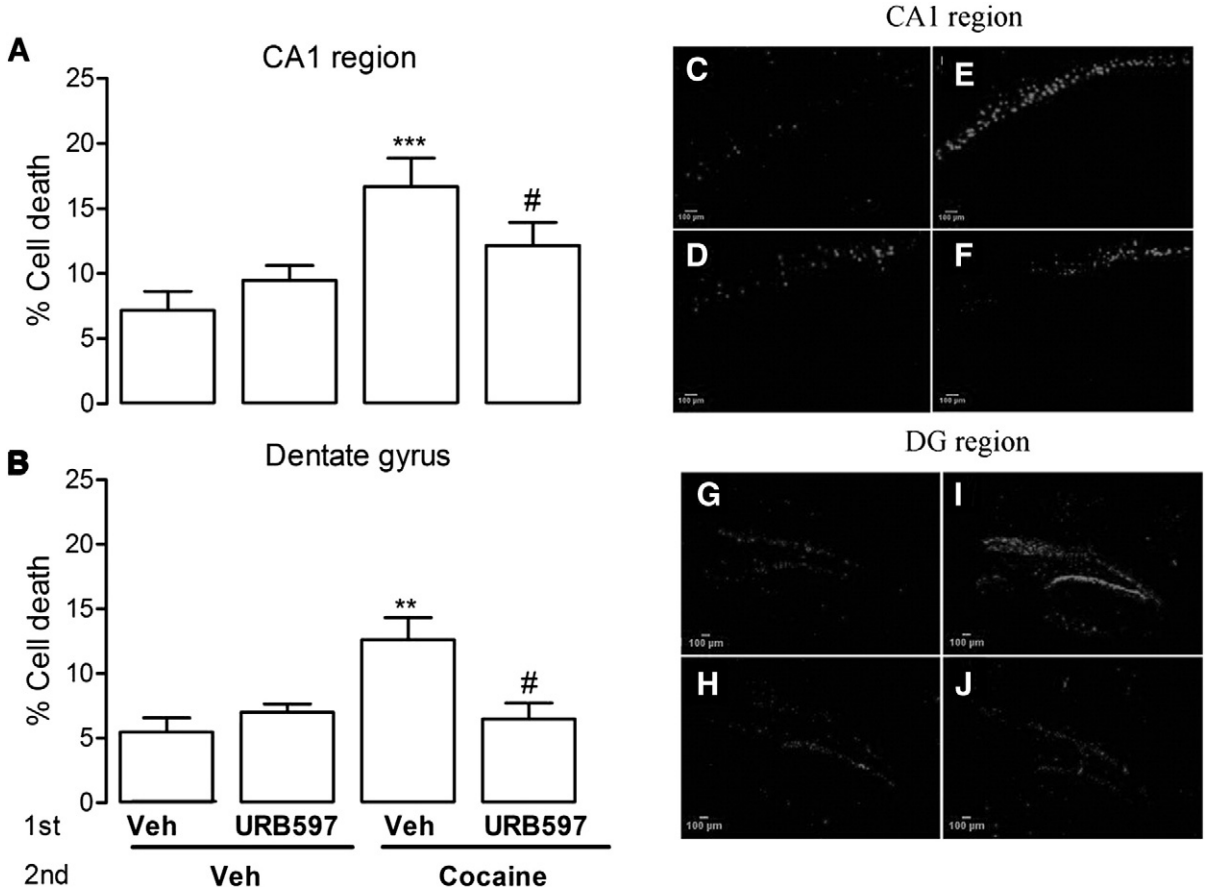

Fig. 5. Effects of the anandamide hydrolysis inhibitor, URB597 (1 mg kg^{-1}), on cocaine (75 mg kg^{-1})-induced cell death the CA1 and dentate gyrus regions of the mouse hippocampus 24 h after the convulsive seizures, as revealed by ethidium homodimer staining. URB597 inhibited cocaine-induced cell death in (A) the CA1 and (B) the dentate gyrus of the hippocampus. Representative photomicrographies of ethidium homodimer stained cells in (C–F) the CA1 and (G–J) the dentate gyrus. Dead cells were indicated by the red fluorescence of ethidium homodimer using 10× magnification. Bar size: 100 µm. $^{**}p < 0.01$ and $^{***}p < 0.001$ compared to vehicle–vehicle (Veh) group; $^{\#}p < 0.05$ compared to Veh + cocaine group; one-way ANOVA followed by Newman–Keuls test. Data are expressed as mean ± SEM (n = 4–6 mice/group).

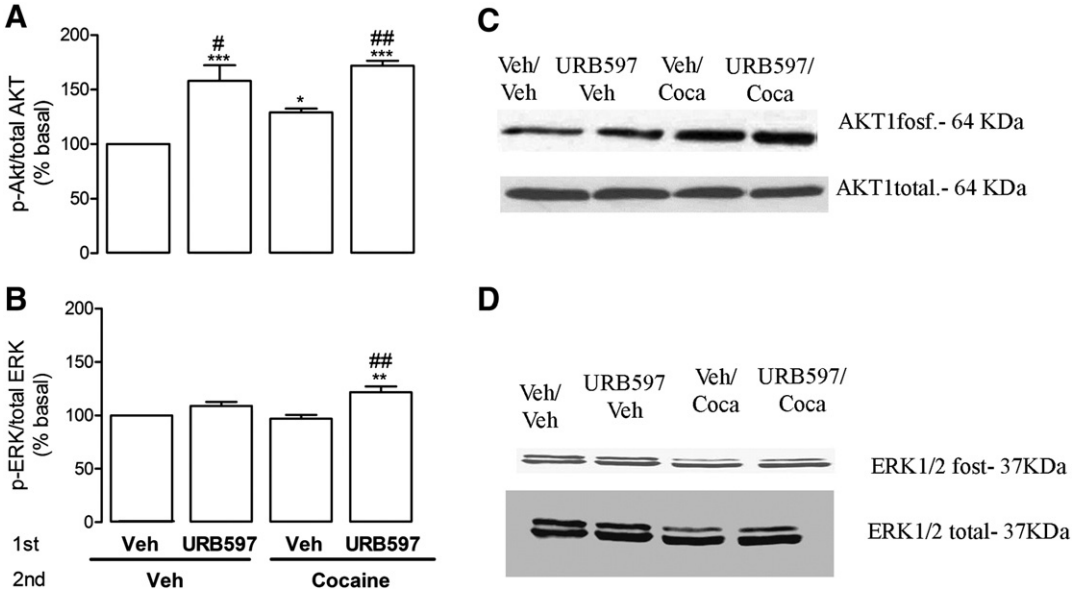

Fig. 6. Effects of URB597 (1 mg kg^{-1}) and cocaine (75 mg kg^{-1}) on the ratio of phosphorylate by total proteins for Akt and ERK1/2. (A) URB597 increased Akt phosphorylation in both vehicle- and cocaine-treated groups, as revealed by densitometric analysis. (B) URB597 selectively increased ERK1/2 phosphorylation in the cocaine-treated group. (C) Representative immunoblots for phospho- (upper panel) and total-Akt expression (lower panel) in hippocampus, as revealed by densitometric analysis. (D) Representative immunoblots for phospho- (upper panel) and total-ERK1/2 expression (lower panel) in hippocampus. $^{*}p < 0.05$ and $^{***}p < 0.001$ compared to vehicle + vehicle (Veh) group; $^{\#}p < 0.05$, $^{\#\#}p < 0.01$ compared to Veh + cocaine group; one-way ANOVA followed by Newman–Keuls test. Data are expressed as mean ± SEM for percentages of basal phosphorylation (n = 4–6 mice/group).

URB597 promotes Akt and ERK phosphorylation in the hippocampus

To assess the contribution of intracellular signaling events to the action of endocannabinoids against cocaine, we determined the phosphorylation pattern of Akt and ERK1/2 in the hippocampus of mice treated with either vehicle or cocaine in the presence or absence of URB597. This FAAH inhibitor increased Akt phosphorylation in both vehicle- and cocaine-treated mice, since there was an overall effect of URB597 ($F_{1,15} = 38.0$, $p < 0.0001$); cocaine also promoted phosphorilation ($F_{1,15} = 6.847$, $p = 0.0194$) and no interaction was observed ($F_{1,15} = 0.8787$, ns) (Fig. 6A). Moreover, URB597 also promoted phosphorylation of ERK1/2 in animals receiving cocaine injection. Again, there was an overall effect of URB597 ($F_{1,15} = 19.60$, $p = 0.0005$), although no cocaine effect was detected ($F_{1,15} = 1.655$, ns). There was, however, an interaction between factors ($F_{1,15} = 4.385$, $p = 0.0436$). Post-hoc analysis revealed that URB597 increase phosphorylation in cocaine treated animals (Fig. 6B). Representative blots are presented in Fig. 6C and D. Drug treatment did not induce changes in total protein expression for both Akt and ERK (data not shown).

URB597 protects against cocaine-induced cell death in hippocampal culture via the CB_1 receptor and PI3K

To clarify the potential mechanisms involved in URB597-mediated effects, we added various concentrations of cocaine to primary cultured hippocampal cells for 20 h. Adding 100 μM to 1000 μM of cocaine resulted in increased cell death compared to vehicle group ($F_{6,21} = 10.95$, $p < 0.0001$; Fig. 7A). To assess if endogenously produced anandamide counteracts cocaine-induced cell death, we incubated the wells with 500 μM cocaine and three concentrations of URB597. Similarly to what we observed in the hippocampus of cocaine-treated animals, this compound reduced the percentage of cell death relative to cocaine ($F_{4,17} = 6.728$, $p = 0.001$; Fig. 7B). To confirm the involvement of CB_1 receptors, we incubated the culture with AM251 (1 nM) together with URB597 (10 nM). The CB_1 receptor antagonist completely reversed the neuroprotective effect of URB597 ($F_{3,17} = 19.13$, $p < 0.0001$; Fig. 7C). Altogether, these findings indicate that cocaine enhances the cell death in hippocampal culture and the URB597 inhibits this effect through CB_1 activation. Finally, considering our own observation that URB597 promoted Akt phosphorylation, we hypothesized that inhibition of PI3K, which is upstream in this signal transduction pathway, mediate the protecting effect of CB_1 receptor activation. Accordingly, the PI3K inhibitor, LY294002 (1 μM), also reversed the protective effect of URB597 ($F_{4,18} = 12.5$, $p < 0.0001$, Fig. 7D). Representative stainings for this experiment are presented in Fig. 8.

Discussion

In the present study, we employed various approaches to test the hypothesis that facilitation of endocannabinoid signaling protects against cocaine neurotoxicity. We performed dose– and concentration–response experiments to select the proper doses of cocaine and the anandamide hydrolysis inhibitor (FAAH inhibitor), URB597. Importantly, this compound was effective against cocaine-induced seizures in mice. This effect possibly occurs through an increase in anandamide action on cannabinoid CB_1 receptor, since the CB_1 selective agonist, ACEA, mimicked this effect and the antagonist, AM251, prevented it. URB597 also reduced cocaine-evoked EEG activity via CB_1 receptor activation. In addition, the anticonvulsant action of URB597 was accompanied by protection against neural activation and death in the hippocampus, along with an increase in the phosphorylation of ERK and Akt survival pathway. The protective effect of FAAH inhibition was confirmed in hippocampal cell culture. Finally, we demonstrated that this action is

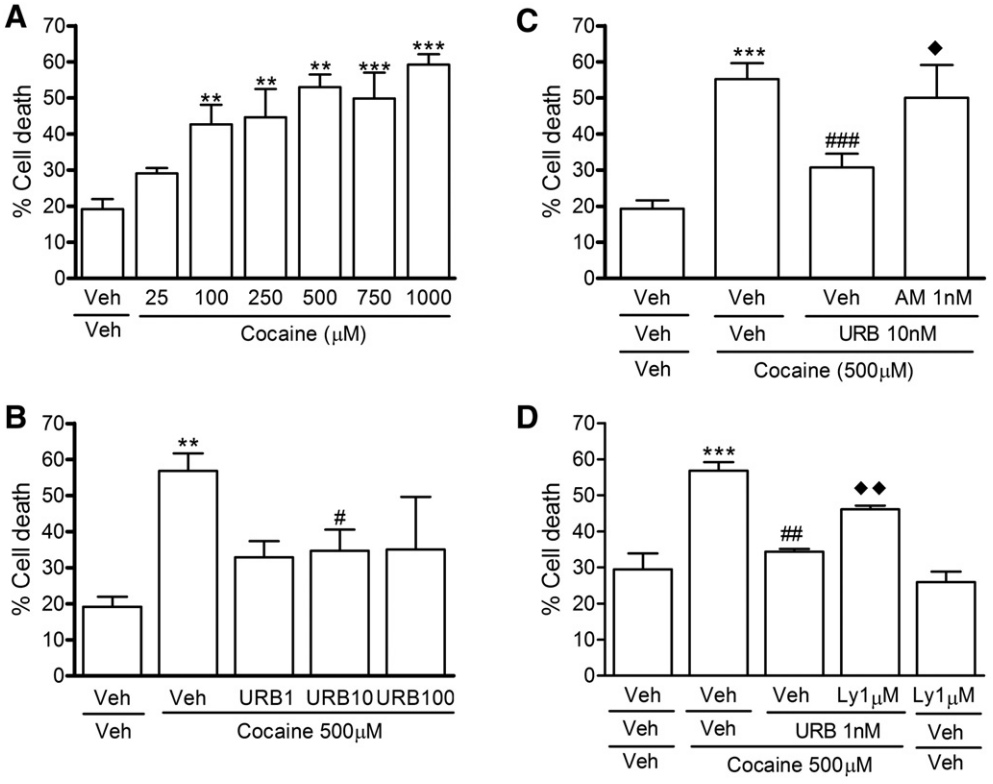

Fig. 7. Effects of URB597 on cocaine-induced death in primary cultured hippocampus and the roles of CB_1 receptor and PI3K. (A) Cocaine increased the percentage of cell death. (B) URB597 inhibited cocaine-induced cell death. (C) The CB_1 receptor antagonist, AM251, reversed the protective effect of URB597. (D) The PI3K inhibitor, LY294002, reversed the protective effect of URB597. $^{**}p < 0.01$ and $^{***}p < 0.001$ compared to the respective vehicle + vehicle (Veh) groups; $^{\#}p < 0.05$ and $^{\#\#\#}p < 0.001$ compared to the respective Veh + cocaine groups; $^{\blacklozenge}p < 0.05$ and $^{\blacklozenge\blacklozenge}p < 0.01$ compared to the respective Veh + URB597 + cocaine groups; one-way ANOVA followed by Newman–Keuls test. Data represent the means ± SEM of three independent experiments.

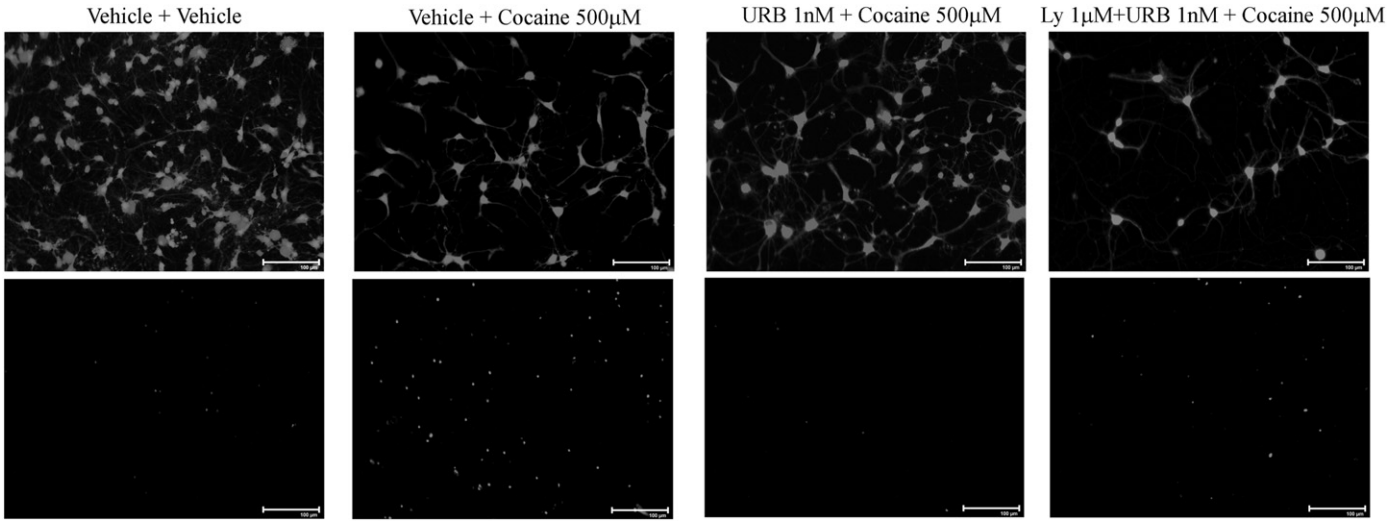

Fig. 8. Representative images for the effects of Veh + Veh + Veh, Veh + Veh + cocaine, Veh + URB597 + cocaine, LY294002 + URB597 + cocaine in primary-cultured hippocampal cells, as revealed by ethidium homodimer-1 labeling. Upper row, calcein AM staining (green, live cells); lower row, ethidium homodimer-1 staining (red, dead cells). Bar size: 100 μm.

mediated by activation of the CB_1 receptor and the PI3K signaling mechanism.

In line with experimental and clinical observations, acute cocaine toxicity was characterized by convulsive seizures and simultaneous electrical spike activity in the EEG (Gasior et al., 1999; Tella et al., 1992). Both inhibition of anandamide hydrolysis and direct activation of the cannabinoid CB_1 receptor prevented these actions. This is in agreement with the potential antiepileptic activity of these compounds. The effects of cannabinoid direct agonists, however, may vary across studies, depending on the dose or model used (Blair et al., 2006; Hofmann and Frazier, 2013; Vilela et al., 2013). In addition, they are more prone to cause side effects, such as motor and memory impairment, as compared to FAAH inhibition. Thus, the later mechanism represents a more reasonable strategy for protecting the brain against various types of noxious stimuli (Moreira and Wotjak, 2010).

The protective effects of compounds that facilitate endocannabinoid activity is in line with studies showing that anandamide modulate seizures by restraining excessive excitatory neurotransmission in certain forebrain regions, particularly the hippocampus (Marsicano et al., 2003; Lutz, 2004; Monory et al., 2006). Both URB597 and ACEA, however, induced bell-shaped effects upon cocaine-induced seizures. Intriguingly, this often occurs with cannabinoid-related compounds in experimental models of anxiety and epileptic seizures. Generally, intermediate doses reduce these responses via CB_1 receptor activation, whereas higher doses induce no effect (Moreira and Wotjak, 2010). One possible explanation for this might be related to the activation of the transient receptor potential vanilloid type-1 (TRPV1) channel. Endogenous anandamide, as well as exogenous cannabinoids, activate TRPV1 channels in the brain, generally resulting in opposite responses as those mediated by CB_1 receptor (Moreira et al, 2012). Thus, the bell-shaped effects of URB597 and ACEA against cocaine-induced seizure may occur due to the balanced activity upon CB_1 and TRPV1 receptors. According to this notion, these compounds would be protective at intermediate doses, through CB_1-mediated mechanisms (as we have shown here), but would have no effects at higher doses, due to simultaneous activation of CB1 and TRPV1 (Moreira and Wotjak, 2010; Moreira et al., 2012). This possibility remains to be confirmed in future experiments.

Regarding the biological bases for URB597 effects, we have focused on the hippocampus due to its proposed role on ictal activity (Oliveira et al., 2011; Kitchigina et al., 2013). Indeed, our data with c-Fos protein expression, a well-established marker of neural activity (Morgan and Curran, 1989), point to specific sub-regions of this structure as the targets for cocaine-induced ictal activity and its reversal by URB597. Based on this result, we investigated cell death in these areas and observed that anandamide hydrolysis inhibition reduced cocaine effects on CA1 and dentate gyrus, in line with the on-demand protective function of endocannabinoid signaling (Fowler et al., 2010). We therefore hypothesized that this effect occurs through activation of the PI3K/Akt/ERK pathway, a neuroprotective mechanism coupled to CB_1 receptor (Ozaita et al., 2007) that promotes cell survival (Dudek et al., 1997; Brunet et al., 2001; Zheng et al., 2002). Indeed, we observed increased phosphorylation of Akt and ERK in the hippocampus of URB597 treated animals. Although the effects upon ERK were subtle, there was a marked increase in Akt phosphorylation. The reason for the apparent discrepancy might be related to the fact that ERK is downstream to Akt in this molecular pathway.

The last series of experiments confirmed these results and established a causal relationship between the PI3K/Akt/ERK pathway activation and the neuroprotective effect of URB597. First, we selected a proper concentration of cocaine for *in vitro* studies by performing a concentration–effect experiment. This is important considering the large variability of cocaine concentrations across different studies (Nassogne et al., 1995, 2004; Poon et al., 2007; Lepsch et al., 2009). In line with previous results, we observed that cocaine promoted cell death at a wild range of concentrations. It remains unclear, however, to which extend these concentrations are representative of *in vivo* neurotoxicity. Moreover, the reasons for the variability in these *in vitro* effects are unclear. In fact, the processes mediating its neurotoxicity have not been clarified (Wiener and Reith, 1990a,b; Planeta et al., 2013). Some apoptotic mechanisms have been implied in this effect, such as tumor necrosis factor TNF-α, the Bax/Bcl2 and caspase pathways (Dey and Snow, 2007; Dey et al., 2007), the nuclear factor NFκB (Lepsch et al., 2009), and the gaseous messenger nitric oxide (Xu et al., 2013).

Having established a neurotoxic concentration of cocaine for our *in vitro* studies, we observed that URB597 conferred protection against cocaine in cell culture, supporting our experiments with live animals. This effect seems to occur via CB_1 receptor activation and the PI3K intracellular pathway, since it was reversed by both AM251 and LY294002. Thus, we identified the CB_1 receptor-mediated recruitment of PI3K as a mechanism responsible for the neuroprotective effect of URB597. This is not necessarily the only signal transduction involved in this process. It represents, however, a logical candidate, since it is coupled to CB_1 receptor and confer protection against excitotoxic stimuli (Xue et al., 2011; Zhang and Wong, 2012).

In conclusion, employing a diversified hypothesis-driven methodology, this study provides evidence that enhancing anandamide actions reduces the neurotoxic effects of cocaine. The molecular process mediating

this effect involves the activation of the CB_1 receptor and the PI3K intracellular survival pathway in the hippocampus. Considering the limited treatments for cocaine intoxication (Connors and Hoffman, 2013), these mechanism may be relevant for the development of new neuroprotective therapeutic strategies based on the endocannabinoid system.

Author's contributions

- All the authors contributed to one of the stages, to the drafting, and the final approval and are accountable for all aspects of this work.
- LRV, PG, TGV, DCM, THFV, JGD and FR performed the research and analyzed the data. LRV conducted most of the experiments as part of his PhD thesis.
- DCA, GSP, ARM, FMR, ACPO, MFDM and FAM supervised the research.
- ACPO, MFDM and FAM designed the study and wrote the final version of the paper, which have been approved by all authors.

Conflicts of interest

The authors declare no conflict of interest.

Transparency Documents

The Transparency documents associated with this article can be found, in the online version.

Acknowledgments

This research received financial support from FAPEMIG (APQ-01728-13), CNPq and INCT-Maq. These funding sources were not involved in any part of this study.

References

Beijamini, V., Guimarães, F.S., 2006. c-Fos expression increase in NADPH-diaphorase positive neurons after exposure to a live cat. Behav. Brain Res. 170, 52–61.
Blair, R.E., Deshpande, L.S., Sombati, S., Falenski, K.W., Martin, B.R., DeLorenzo, R.J., 2006. Activation of the cannabinoid type-1 receptor mediates the anticonvulsant properties of cannabinoids in the hippocampal neuronal culture models of acquired epilepsy and status epilepticus. J. Pharmacol. Exp. Ther. 317, 1072–1078.
Brunet, A., Datta, S.R., Greenberg, M.E., 2001. Transcription-dependent and -independent control of neuronal survival by the PI3K-Akt signalling pathway. Curr. Opin. Neurobiol. 11, 297–305.
Cadet, J.L., Bisagno, V., Milroy, C.M., 2014. Neuropathology of substance use disorders. Acta Neuropathol. 127, 91–107.
Connors, N.J., Hoffman, R.S., 2013. Experimental treatments for cocaine toxicity: a difficult transition to the bedside. J. Pharmacol. Exp. Ther. 347, 251–257.
Cravatt, B.F., Giang, D.K., Mayfield, S.P., Boger, D.L., Lerner, R.A., Gilula, N.B., 1996. Molecular characterization of an enzyme that degrades neuromodulatory fatty-acid amides. Nature 384, 82–87.
Cunha-Oliveira, T., Rego, A.C., Oliveira, C.R., 2008. Cellular and molecular mechanisms involved in the neurotoxicity of opioid and psychostimulant drugs. Brain Res. Rev. 58, 192–208.
Degenhardt, L., Hall, W., 2012. Extent of illicit drug use and dependence, and their contribution to the global burden of disease. Lancet 379, 55–70.
Dey, S., Snow, D.M., 2007. Cocaine exposure *in vitro* induces apoptosis in fetal locus coeruleus neurons through TNF-alpha-mediated induction of Bax and phosphorylated c-Jun NH(2)-terminal kinase. J. Neurochem. 103, 542–556.
Dey, S., Mactutus, C.F., Booze, R.M., Snow, D.M., 2007. Cocaine exposure *in vitro* induces apoptosis in fetal locus coeruleus neurons by altering the Bax/Bcl-2 ratio and through caspase-3 apoptotic signalling. Neuroscience 144, 509–521.
Doria, J.G., Silva, F.R., de Souza, J.M., Vieira, L.B., Carvalho, T.G., Reis, H.J., et al., 2013. Metabotropic glutamate receptor 5 positive allosteric modulators are neuroprotective in a mouse model of Huntington's disease. Br. J. Pharmacol. 169, 909–921.
Dudek, H., Datta, S.R., Franke, T.F., Birnbaum, M.J., Yao, R., Cooper, G.M., et al., 1997. Regulation of neuronal survival by the serine-threonine protein kinase Akt. Science 275, 661–665.
Fowler, C.J., Rojo, M.L., Rodriguez-Gaztelumendi, A., 2010. Modulation of the endocannabinoid system: neuroprotection or neurotoxicity? Exp. Neurol. 224, 37–47.
Galve-Roperh, I., Rueda, D., Gómez del Pulgar, T., Velasco, G., Guzmán, M., 2002. Mechanism of extracellular signal-regulated kinase activation by the CB(1) cannabinoid receptor. Mol. Pharmacol. 62, 1385–1392.
Gasior, M., Ungard, J.T., Witkin, J.M., 1999. Preclinical evaluation of newly approved and potential antiepileptic drugs against cocaine-induced seizures. J. Pharmacol. Exp. Ther. 290, 1148–1156.
Hayase, T., Yamamoto, Y., Yamamoto, K., 2001. Protective effects of cannabinoid receptor agonists against cocaine and other convulsant-induced toxic behavioural symptoms. J. Pharm. Pharmacol. 53, 1525–1532.
Heard, K., Cleveland, N.R., Krier, S., 2011. Benzodiazepines and antipsychotic medications for treatment of acute cocaine toxicity in animal models–a systematic review and meta-analysis. Hum. Exp. Toxicol. 30, 1849–1854.
Hofmann, M.E., Frazier, C.J., 2013. Marijuana, endocannabinoids, and epilepsy: potential and challenges for improved therapeutic intervention. Exp. Neurol. 244, 43–50.
Karanian, D.A., Karim, S.L., Wood, J.T., Williams, J.S., Lin, S., Makriyannis, A., et al., 2007. Endocannabinoid enhancement protects against kainic acid-induced seizures and associated brain damage. J. Pharmacol. Exp. Ther. 322, 1059–1066.
Kathuria, S., Gaetani, S., Fegley, D., Valiño, F., Duranti, A., Tontini, A., et al., 2003. Modulation of anxiety through blockade of anandamide hydrolysis. Nat. Med. 9, 76–81.
Kishi, T., Matsuda, Y., Iwata, N., Correll, C.U., 2013. Antipsychotics for cocaine or psychostimulant dependence: systematic review and meta-analysis of randomized, placebo-controlled trials. J. Clin. Psychiatry 74, e1169–e1180.
Kitchigina, V., Popova, I., Sinelnikova, V., Malkov, A., Astasheva, E., Shubina, L., Aliev, R., 2013. Disturbances of septohippocampal theta oscillations in the epileptic brain: reasons and consequences. Exp. Neurol. 247, 314–327.
Koob, G.F., Nestler, E.J., 1997. The neurobiology of drug addiction. J. Neuropsychiatry Clin. Neurosci. 9, 482–497.
Leite, H.R., Mourão, F.A., Drumond, L.E., Ferreira-Vieira, T.H., Bernardes, D., Silva, J.F., et al., 2012. Swim training attenuates oxidative damage and promotes neuroprotection in cerebral cortical slices submitted to oxygen glucose deprivation. J. Neurochem. 123, 317–324.
Lepsch, L.B., Munhoz, C.D., Kawamoto, E.M., Yshii, L.M., Lima, L.S., Curi-Boaventura, M.F., et al., 2009. Cocaine induces cell death and activates the transcription nuclear factor kappa-B in PC12 cells. Mol. Brain 2, 3.
Lutz, B., 2004. On-demand activation of the endocannabinoid system in the control of neuronal excitability and epileptiform seizures. Biochem. Pharmacol. 68, 1691–1698.
Marsicano, G., Goodenough, S., Monory, K., Hermann, H., Eder, M., Cannich, A., et al., 2003. CB1 cannabinoid receptors and on-demand defense against excitotoxicity. Science 302, 84–88.
Monory, K., Massa, F., Egertová, M., Eder, M., Blaudzun, H., Westenbroek, R., et al., 2006. The endocannabinoid system controls key epileptogenic circuits in the hippocampus. Neuron 51, 455–466.
Moreira, F.A., Wotjak, C.T., 2010. Cannabinoids and anxiety. Curr. Top. Behav. Neurosci. 2, 429–450.
Moreira, F.A., Aguiar, D.C., Terzian, A.L., Guimarães, F.S., Wotjak, C.T., 2012. Cannabinoid type 1 receptors and transient receptor potential vanilloid type 1 channels in fear and anxiety-two sides of one coin? Neuroscience 204, 186–192.
Moreira, F.A., Jupp, B., Belin, D., Dalley, J.W., 2015. Endocannabinoids and striatal function, implications for addiction-related behaviours. Behav. Pharmacol. 26, 59–72.
Morgan, J.I., Curran, T., 1989. Stimulus-transcription coupling in neurons: role of cellular immediate-early genes. Trends Neurosci. 12, 459–462.
Nassogne, M.C., Evrard, P., Courtoy, P.J., 1995. Selective neuronal toxicity of cocaine in embryonic mouse brain cocultures. Proc. Natl. Acad. Sci. U. S. A. 92, 11029–11033.
Nassogne, M.C., Lizarraga, C., N'Kuli, F., Van Bambeke, F., Van Binst, R., Wallemacq, P., Tulkens, P.M., Mingeot-Leclercq, M.P., Levade, T., Courtoy, P.J., 2004. Cocaine induces a mixed lysosomal lipidosis in cultured fibroblasts, by inactivation of acid sphingomyelinase and inhibition of phospholipase A1. Toxicol. Appl. Pharmacol. 194, 101–110.
Oliveira, M.S., Pacheco, L.F., Mello, C.F., Cavalheiro, E.A., Garrido-Sanabria, E.R., 2011. Epileptiform activity in the limbic system. Front. Biosci. Schol. Ed. 3, 565–593.
Ozaita, A., Puighermanal, E., Maldonado, R., 2007. Regulation of PI3K/Akt/GSK-3 pathway by cannabinoids in the brain. J. Neurochem. 102, 1105–1114.
Panlilio, L.V., Justinova, Z., Goldberg, S.R., 2010. Animal models of cannabinoid reward. Br. J. Pharmacol. 160, 499–510.
Paxinos, G., Watson, C., 1997. The Mouse Brain in Stereotaxic Coordinates. Academic Press, New York.
Piomelli, D., 2003. The molecular logic of endocannabinoid signalling. Nat. Rev. Neurosci. 4, 873–884.
Planeta, C.S., Lepsch, L.B., Alves, R., Scavone, C., 2013. Influence of the dopaminergic system, CREB, and transcription factor-κB on cocaine neurotoxicity. Braz. J. Med. Biol. Res. 46, 909–915.
Poon, H.F., Abdullah, L., Mullan, M.A., Mullan, M.J., Crawford, F.C., 2007. Cocaine-induced oxidative stress precedes cell death in human neuronal progenitor cells. Neurochem. Int. 50, 69–73.
Ribeiro, F.M., Paquet, M., Ferreira, L.T., Cregan, T., Swan, P., Cregan, S.P., et al., 2010. Metabotropic glutamate receptor-mediated cell signalling pathways are altered in a mouse model of Huntington's disease. J. Neurosci. 30, 316–324.
Slusar, J.E., Cairns, E.A., Szczesniak, A.M., Bradshaw, H.B., Di Polo, A., Kelly, M.E., 2013. The fatty acid amide hydrolase inhibitor, URB597, promotes retinal ganglion cell neuroprotection in a rat model of optic nerve axotomy. Neuropharmacology 72, 116–125.
Tella, S.R., Korupolu, G.R., Schindler, C.W., Goldberg, S.R., 1992. Pathophysiological and pharmacological mechanisms of acute cocaine toxicity in conscious rats. J. Pharmacol. Exp. Ther. 262, 936–946.
van der Stelt, M., Di Marzo, V., 2005. Cannabinoid receptors and their role in neuroprotection. NeuroMolecular Med. 7, 37–50.
Vilela, L.R., Medeiros, D.C., Rezende, G.H., de Oliveira, A.C., Moraes, M.F., Moreira, F.A., 2013. Effects of cannabinoids and endocannabinoid hydrolysis inhibition on pentylenetetrazole-induced seizures and electroencephalographic activity in rats. Epilepsy Res. 104, 195–202.
Vilela, L.R., Medeiros, D.C., de Oliveira, A.C., Moraes, M.F., Moreira, F.A., 2014. Anticonvulsant effects of N-arachidonoyl-serotonin, a dual FAAH enzyme and TRPV1 channel

blocker, on experimental seizures: the roles of cannabinoid CB1 receptors and TRPV1 channels. Basic Clin. Pharmacol. Toxicol. 115, 330–334.
Wiener, H.L., Reith, M.E., 1990a. Correlation between cocaine-induced locomotion and cocaine disposition in the brain among four inbred strains of mice. Pharmacol. Biochem. Behav. 36, 699–701.
Wiener, H.L., Reith, M.E., 1990b. Correlation between cocaine-induced locomotion and cocaine disposition in the brain among four inbred strains of mice. Pharmacol. Biochem. Behav. 36, 699–701.
Wise, R.A., 1984. Neural mechanisms of the reinforcing action of cocaine. NIDA Res. Monogr. 50, 15–33.
Xi, Z.X., Gardner, E.L., 2008. Hypothesis-driven medication discovery for the treatment of psychostimulant addiction. Curr. Drug Abuse Rev. 1, 303–327.
Xu, R., Serritella, A.V., Sen, T., Farook, J.M., Sedlak, T.W., Baraban, J., et al., 2013. Behavioral effects of cocaine mediated by nitric oxide-GAPDH transcriptional signalling. Neuron 78, 623–630.
Xue, Y., Xie, N., Lin, Y., Xu, J., Han, Y., Wang, S., et al., 2011. Role of PI3K/Akt in diazoxide preconditioning against rat hippocampal neuronal death in pilocarpine-induced seizures. Brain Res. 1383, 135–140.
Zhang, B., Wong, M., 2012. Pentylenetetrazole-induced seizures cause acute, but not chronic, mTOR pathway activation in rat. Epilepsia 53, 506–511.
Zheng, W.H., Kar, S., Quirion, R., 2002. Insulin-like growth factor-1-induced phosphorylation of transcription factor FKHRL1 is mediated by phosphatidylinositol 3-kinase/Akt kinase and role of this pathway in insulin-like growth factor-1-induced survival of cultured hippocampal neurons. Mol. Pharmacol. 62, 225–233.